ACS OMEGA

Open Access

http://pubs.acs.org/journal/acsodf

Article

Fucoxanthin Ameliorates Kidney Injury by CCl_4-Induced via Inhibiting Oxidative Stress, Suppressing Ferroptosis, and Modulating Gut Microbiota

Yaping Ding, Jiena Ye, Ying Liu, Shaohua Zhang, Yan Xu, Zuisu Yang,* and Zhongliang Liu*

Cite This: *ACS Omega* 2025, 10, 7407−7421

Read Online

ACCESS | Metrics & More | Article Recommendations

ABSTRACT: Chemical-induced kidney injury represents a substantial health risk, with ferroptosis, a type of cell death caused by lipid peroxidation, playing a role in numerous kidney ailments. Fucoxanthin (Fx), a natural carotenoid known for its antioxidant capabilities, has shown promise in alleviating renal injury, but its exact mechanisms are yet to be fully understood. Carbon tetrachloride (CCl_4) is recognized as a powerful nephrotoxic substance, and this study explores the therapeutic effects of Fx on oxidative stress, ferroptosis and intestinal microbiota in mouse kidneys subjected to CCl_4 exposure. The mice were randomly assigned to control, model, colchicine groups (0.1 mg/kg/d), and Fx (50, 100 mg/kg/d) group and underwent related treatments for 4 weeks. Then, we evaluated their renal function, histological alterations in the kidneys, colon, and jejunum, and the levels of related proteins (i.e., Nrf2, GPX4, SLC7A11, HO-1, TFR1, NQO1, GCLM, FTL). Additionally, their gut microbiota was analyzed using 16S rRNA gene sequencing. The results showed that compared to the CCl_4 group, Fx treatment led to lower serum creatinine and blood urea nitrogen levels, reduced malondialdehyde activity in kidneys and intestinal tissues, and increased activity of antioxidant enzymes. Fx also reduced dysbiosis and enhanced the diversity of intestinal flora. In summary, Fx reduced oxidative stress and ferroptosis and partially restored intestinal bacteria, thus improving CCl_4-induced renal damage in mice. These results suggest Fx as a potential therapeutic option for kidney injuries related to oxidative stress. Further research is needed to clarify its precise mechanisms and potential clinical implications.

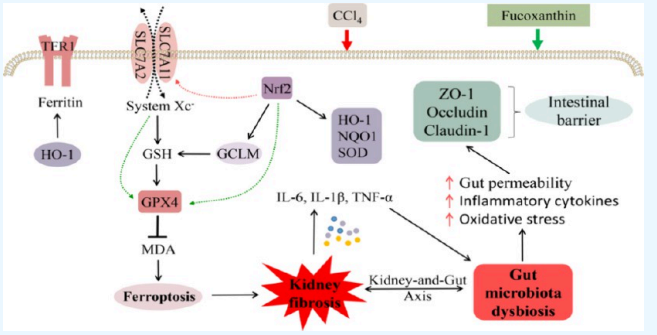

1. INTRODUCTION

Kidney disease, which includes both acute kidney injury and chronic kidney disease, presents a substantial global public health challenge due to its elevated morbidity and mortality rates.[1] A critical aspect of chronic kidney disease pertains to the bidirectional crosstalk between the intestines and the kidneys,[2] where intestinal dysbiosis, characterized by microbial imbalance and compromised barrier integrity, assumes a prominent role.[3]

Recent studies indicate that several drugs can modulate the intestine to enhance renal function. Notable examples include the isolation of bacterial endotoxins by resveratrol to improve diabetic nephropathy[4]; protection against intestinal flora dysbiosis and renal injury by resveratrol butyrate;[5] and the amelioration of intestinal barrier dysfunction and diabetic kidney injury by Punicalagin,[6] thereby highlighting the intricate interplay between the intestine and the kidneys.[7,8]

Ferroptosis, a nonapoptotic form of cell death characterized by iron-dependent lipid peroxide accumulation, has been identified as a crucial mechanism in both chronic[9] and acute kidney injury.[10,11] Strategies aimed at targeting ferroptosis[12] have proven effective in reducing kidney injury[13] and ameliorating renal fibrosis,[14] through the use of drugs such as quercetin,[15] tectorigenin,[16] nobiletin, liproxstatin-1,[17,18] and melatonin.[19] Given the connection between kidney disease and ferroptosis, it represents an important therapeutic target.While existing treatments for kidney disease, such as those modulating the gut-kidney axis or targeting ferroptosis, show promise, they often have limitations or adverse effects.This highlights the need for safer and more effective therapeutic options. Fucoxanthin (Fx), a carotenoid specific to algae and known for its antioxidant and anti-inflammatory properties,[20,21] has exhibited potential in restoring renal function[22] and preventing kidney fibrosis,[23,24] as well as mitigating intestinal inflammation.[25] Unlike the drugs mentioned above,

Received: December 27, 2024
Revised: January 31, 2025
Accepted: February 4, 2025
Published: February 14, 2025

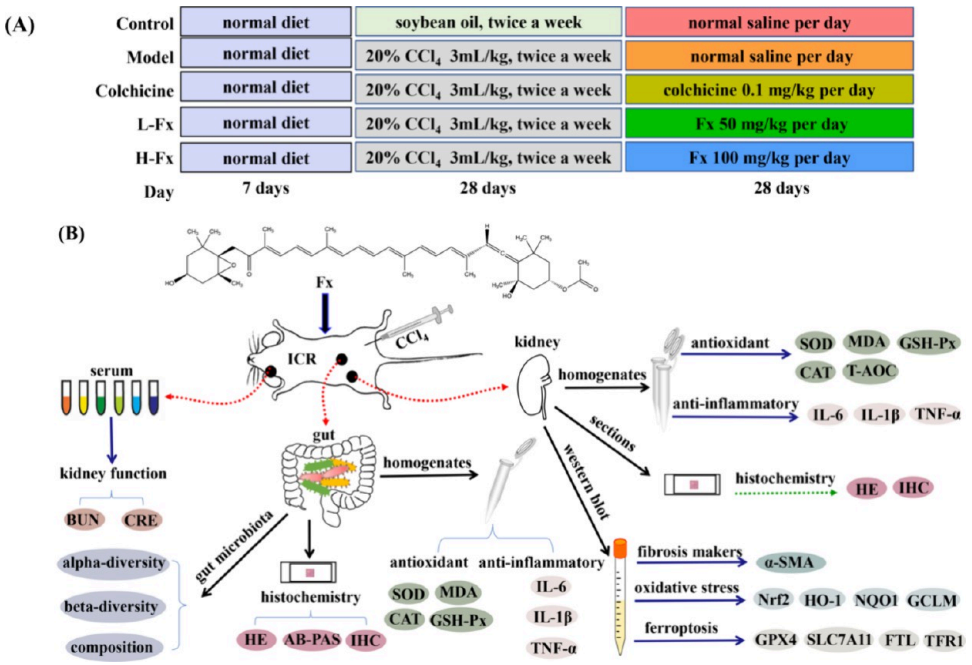

Figure 1. (A) Research protocol for inducing kidney injury mice, and (B) assessments (n = 9).

which focus on modulating the gut microbiome or inhibiting specific inflammatory pathways, Fx's multifaceted approach-targeting both oxidative stress and intestinal health-may offer a unique advantage. Studies using CCl_4 to induce kidney injury in mouse models have reported disruptions in intestinal tight junction proteins and microbial imbalance[26,27] demonstrating the close relationship between kidney function and gut health.[28,29]

In this current study, we address an existing knowledge gap by examining the impact of Fx on CCl_4-induced kidney injury, with a particular emphasis on GPX4-mediated ferroptosis and the intestinal-renal axis. Our findings suggest that Fx may offer a novel therapeutic strategy by simultaneously modulating oxidative stress, intestinal health, and renal function, positioning it as a promising candidate for future kidney disease treatments.

2. MATERIALS AND METHODS

2.1. Animals and Experimental Design. Fx, with a purity of 70%, with the remaining 30% containing lipids, sterols, low concentration of chlorophyll, and water, was obtained from Shandong Jiejing Group Corporation (Shandong, China). While colchicine (SFDA approval number: H53021534, batch number: 1904A) was purchased from KPC Pharmaceuticals, Inc. Male ICR mice, aged 6−8 weeks and weighing 20 ± 2 g, were selected for this study. The source and housing conditions of the ICR mice were consistent with previous research.[63] After a one-week acclimation period, the experimental protocol was implemented as follows: Nine mice were randomly assigned to the control group and received biweekly injections of soybean oil. Conversely, the remaining 36 mice were administered biweekly injections of CCl_4 (3 mL/kg, 20% CCl_4) for 4 weeks to induce renal injury.

Upon successful model establishment, the mice were randomly divided into four groups: (1) Model group: received daily administration of normal saline; (2) Colchicine group: given daily dosage of 0.1 mg/kg; (3) Low-Dose Fx (L-Fx) group: administered daily dosage of 50 mg/kg; (4) High-Dose Fx (H-Fx) group: received daily dosage of 100 mg/kg. The mice were observed daily throughout the intervention period, and upon completion of the study, the animals were humanely euthanized, their weights were recorded, and their tissues (renal, colon, and jejunum) were fixed in 4% paraformaldehyde. Additionally, cecal contents were stored at −80 °C. Figure 1A and B provide a visual representation of the experimental design and the workflow for kidney injury assessment and subsequent analyses. Our research protocol strictly adhered to ethical guidelines and was approved by our institutional review board.

2.2. Analysis of Renal Function. After a 4-week intervention with Fx, blood samples were obtained from 45 mice and centrifuged at 8000 rpm and 4 °C for 10 min to isolate the serum for biochemical analysis. The analysis of CRE (C011-2-1) and BUN (C013-2-1) levels in the serum was performed using their respective assay kits following the manufacturer's instructions to obtain valuable insights into the renal function of animals from different groups.

2.3. Analysis of Antioxidants and Lipid Peroxides. Tissues from the kidney, colon and jejunum (200 mg each) were immersed in 1800 μL of normal saline and then homogenized at 4 °C. The supernatants were collected after centrifugation at 4000 rpm for 10 min and utilized for the analysis of CAT (A007-1-1), SOD (A001-2-1), MDA (A003-1-2), T-AOC (A015-3-1), and GSH-Px (A005-1-2) activities using their respective assay kits. The total protein content in the tissue homogenate was quantified using the bicinchoninic acid assay for the normalization of enzymatic activities.

2.4. Determination of Proinflammatory Cytokines. Following the procedures outlined in Section 2.3, homogenates were prepared using saline. The quantification of IL-1β (KE10003), TNF-α (KE10002), and IL-6 (KE10007) levels was conducted utilizing ELISA kits.

2.5. Histological Analysis. After 4 weeks of Fx treatment, kidney, colon and jejunum samples from each group were embedded in paraffin following standard procedures, sectioned

https://doi.org/10.1021/acsomega.4c11437
ACS Omega 2025, 10, 7407−7421

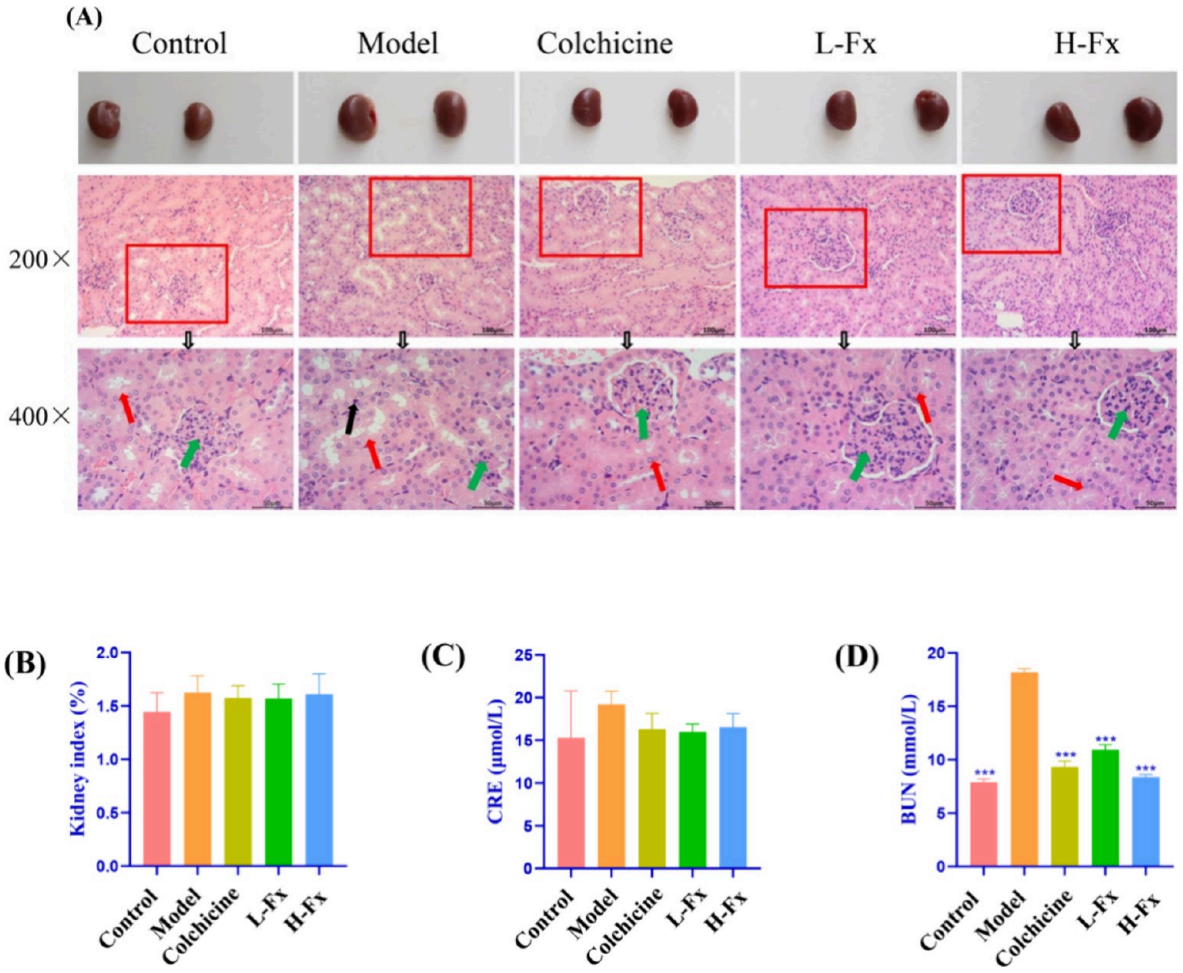

Figure 2. Kidney injury in mice. (A) Hematoxylin and eosin (H&E) staining of kidney tissues (×200, scale bar is 100 μm, ×400, scale bar is 50 μm). (B) Kidney index of mice (n = 9). (C) Creatinine (CRE) and (D) blood urea nitrogen (BUN) contents in the serum of mice (n = 9). Glomeruli (↑), tubules (↑), and inflammatory cells (↑). *** $p < 0.001$ vs carbon tetrachloride (CCl_4) group.

into 4 μm thick slices and subjected to histological analysis using H&E (C0105S) staining. The presence of glycogen in colonic tissue was assessed using AB-PAS (D033-1-1) staining. Photomicrographs of the H&E and AB-PAS stained sections were acquired using an optical microscope.

2.6. Immunochemistry. IHC, utilizing materials from Boster Biological Technology Co. Ltd., was employed to assess the expression location and intensity of related proteins. The expression levels of Nrf2 (16396-1-AP, 1:200) and GPX4 (14432-1-AP, 1:200) proteins in the kidneys were quantified through IHC. Similarly, IHC was conducted to evaluate the expression of ZO-1 (6512254, 1:100), Occludin (53t8241, 1:100) and Claudin-1 (83c6911, 1:100) proteins in the colon and jejunum. Finally, images were captured under a light microscope and analyzed semiquantitatively using the ImageJ 1.53f51 software.

2.7. Western Blot Analysis. The lysis buffer, composed of RIPA and PMSF solution at a ratio of 100:1, was used to lyse the renal tissues. Subsequently, the lysate was centrifuged at 4 °C, 10,000g for 10 min, and the resulting supernatant was collected. An equal volume of protein and 6× SDS loading buffer were added to the supernatant, and the solution was then boiled for 10 min. The protein was subjected to electrophoresis using varying concentrations of SDS-PAGE, followed by transfer to polyvinylidene difluoride membranes. After blocking for 1 h, the membranes were incubated overnight at 4 °C with primary antibodies targeting α-SMA (14395-1-AP, 1:2000), Nrf2 (1:1000), HO-1 (66743-1-Ig, 1:2000), TFR1 (10084-2-AP, 1:1000), FTL (10727-1-AP, 1:2000), SLC7A11 (26864-1-AP, 1:1000), NQO1 (67240-1-Ig, 1:2000), GPX4 (1:1000), GCLM (14241-1-AP, 1:2000), and GAPDH, respectively. Following this, the membranes were incubated with the corresponding secondary antibodies for 1 h. A chemiluminescence system was used to visualize the proteins, which were quantified using the Alpha View 3.4.0.728 software.

2.8. 16S rRNA Gene Sequencing. The CTAB/SDS method, consistent with our laboratory's previous protocol,[26] was used for extracting DNA from the cecal contents of the mice. The amplification of 16S rRNA gene sequences was conducted using the forward primer 338F (5′-ACTCC-TACGGGAGGCAGCAG-3′) and the reverse primer 806R (5′-GGACTACHVGGGTWTCTAA-3′) targeting the V3−V4 regions. All PCR reactions were subjected to 30 thermal cycles in a 30 μL reaction volume, following the specified procedure. Subsequently, the presence of the desired amplified DNA fragments was confirmed by 2% agarose gel electrophoresis. Purification of the mixed PCR products was conducted using the GeneJET Gel Extraction Kit (Thermo Scientific). Sequencing libraries comprising 250 bp paired-end reads

https://doi.org/10.1021/acsomega.4c11437
ACS Omega 2025, 10, 7407−7421

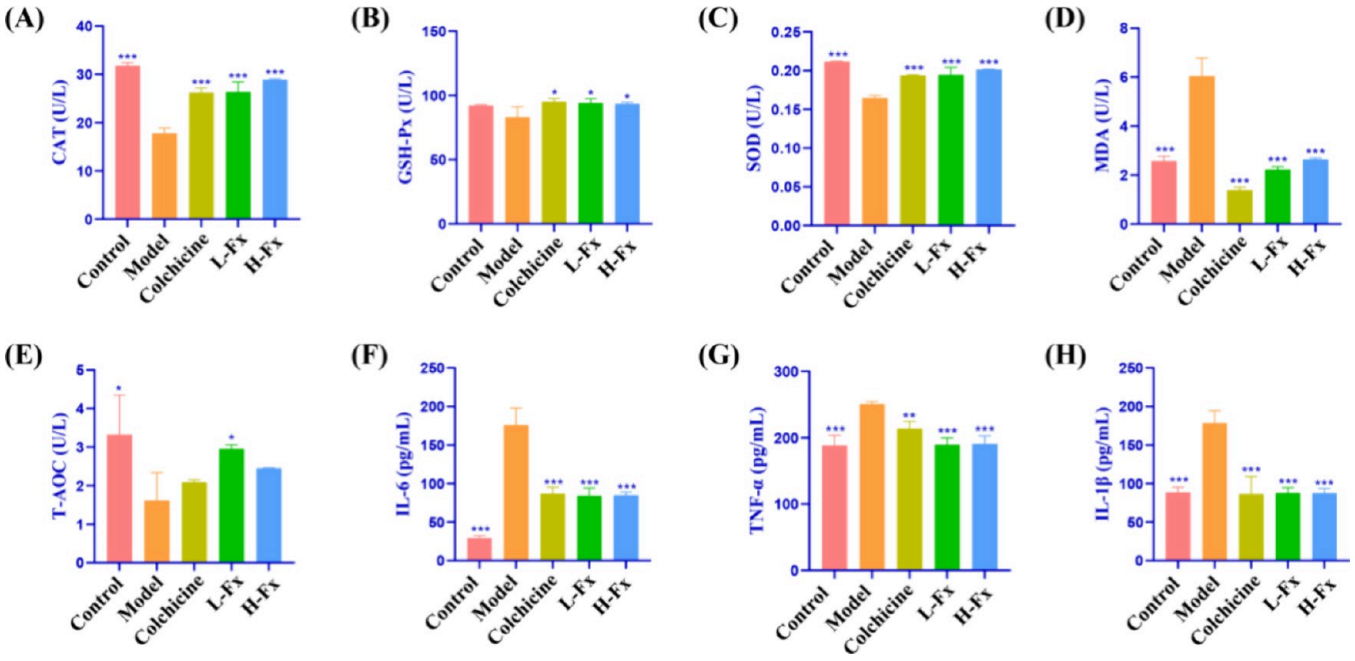

Figure 3. Levels of (A) catalase (CAT), (B) glutathione peroxidase (GSH-Px), (C) superoxide dismutase (SOD), (D) malondialdehyde (MDA), (E) total antioxidant capacity (T-AOC), (F) interleukin-6 (IL-6), (G) tumor necrosis factor-α (TNF-α), and (H) interleukin-1β (IL-1β) in mice kidneys (n = 9). ** $p < 0.01$, *** $p < 0.001$ vs CCl_4 group.

were generated using the NEB Next Ultra DNA Library Prep Kit for Illumina (NEB, USA).

2.9. Sequencing Data Analysis. Paired-end reads were allocated to their respective samples based on unique barcodes. OTUs were defined at a 97% similarity level using UPARSE software, which grouped sequences with similar identity into distinct OTUs. Community diversity analyses, which include both alpha and beta diversity, as well as clustering analyses, were performed using QIIME. Differences in the abundance of specific taxa between the two groups were assessed using the Meta stats software. Furthermore, within different groups, LEfSe was employed for quantitative biomarker analysis. Lastly, a comprehensive statistical assessment of the microbial community's structure and composition was conducted at various taxonomic levels to systematically explore the correlations between intestinal flora and renal indicators, contributing to a deeper understanding of the intricate interrelationships involved.

2.10. Statistical Analysis. Statistical analyses comparing groups were performed using one-way ANOVA conducted with GraphPad Prism 8.3.0 software. The results are presented as means ± standard errors of the means, and significance was defined as p-values less than 0.05. Specifically, $p < 0.05$ indicates statistically significant differences, while $p < 0.001$ denotes exceptionally significant distinctions.

3. RESULTS

3.1. Kidney Histomorphometry, Renal Indices and Renal Function Indices in Mice. The pathological effects of CCl_4-induced renal injury in mice were assessed by evaluating kidney morphology, performing histopathological staining with hematoxylin and eosin (H&E), and measuring serum levels of creatinine (CRE) and blood urea nitrogen (BUN), which are important indicators of renal function. As shown in Figure 2A, the kidneys in the CCl_4-exposed group exhibited significant pathological enlargement compared to the control group, which both colchicine and Fx treatments could significantly mitigate. H&E staining confirmed Fx's capacity to attenuate CCl_4-induced damage such as glomerular atrophy, narrowing or obstruction of the renal capsule lumen, proximal tubular edema and interstitial fibrosis (Figure 2A). Notably, there were no significant differences observed in renal index and CRE levels between the groups (Figure 2B,C). However, BUN levels were significantly increased in the CCl_4-exposed group (18.20 ± 0.33) compared to the control group (7.90 ± 0.30) but significantly reduced in both the colchicine (9.34 ± 0.52) and Fx (8.37 ± 0.26) treatment groups (Figure 2D, $p < 0.001$). These findings indicate that Fx may protect against CCl_4-induced nephrotoxicity by alleviating both functional and morphological abnormalities in the kidneys, thereby supporting Fx as a potential therapeutic candidate for alleviating renal injury associated with exposure to toxic substances.

3.2. Antioxidant Enzymes, Lipid Peroxidation and Inflammatory Factors in Mouse Kidney. We assessed the impact of CCl_4 exposure on enzymatic antioxidant defenses and proinflammatory cytokine levels, as well as the therapeutic efficacy of colchicine, L-Fx, and H-Fx treatments.

All treatments significantly improved antioxidant enzyme activities compared to the CCl_4-exposed group, with Fx showing comparable or superior efficacy to colchicine. Specifically, catalase (CAT) activity, which decreased significantly in the CCl_4-exposed group, was restored by colchicine and both Fx treatments ($p < 0.001$, Figure 3A). Glutathione peroxidase (GSH-Px) activity showed a nonsignificant decrease in the CCl_4 group, but all treatments significantly improved GSH-Px levels compared to the CCl_4-exposed group ($p < 0.05$, Figure 3B). Superoxide dismutase (SOD) activity, which decreased significantly in the CCl_4 group, was increased to near-normal levels in all treatment groups ($p < 0.001$, Figure 3C). Malondialdehyde (MDA) levels, elevated in the CCl_4 group, were significantly reduced in all Fx-treated groups ($p < 0.001$, Figure 3D). Total antioxidant capacity (T-AOC) was

https://doi.org/10.1021/acsomega.4c11437
ACS Omega 2025, 10, 7407−7421

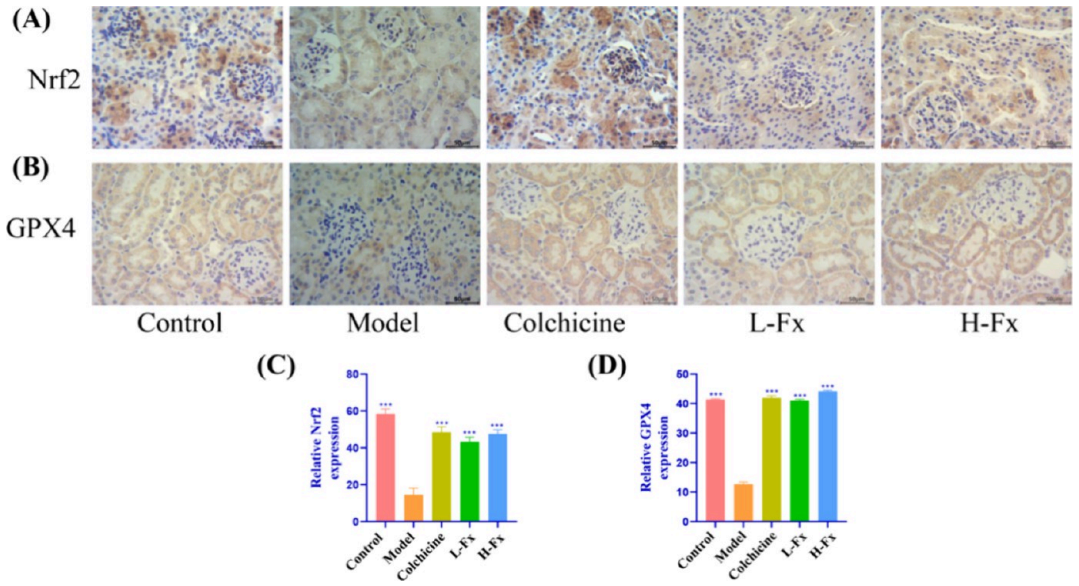

Figure 4. Expression of nuclear factor erythroid 2-related factor 2 (Nrf2), and peroxidase 4 (GPX4) proteins in mice kidneys (×400, scale bar is 50 μm). Expression of (A) Nrf2 and (B) GPX4 analyzed by immunochemistry (IHC). (C) Nrf2 and (D) GPX4 protein levels (n = 3). ***p < 0.001 vs CCl_4 group.

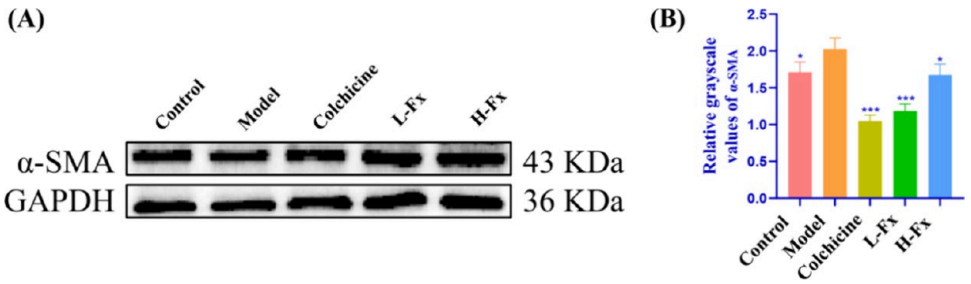

Figure 5. Expression of kidney fibrosis marker protein in mice kidneys. (A) Western blot analysis of alpha-smooth muscle actin (α-SMA) expression. (B) Protein levels of α-SMA (n = 3). **p < 0.01, ***p < 0.001 vs CCl_4 group.

significantly lower in the CCl_4 group, while the L-Fx group showed a significant increase (p < 0.05, Figure 3E).

Regarding proinflammatory cytokines, Fx and colchicine significantly reduced levels of IL-6, TNF-α, and IL-1β, indicating a strong anti-inflammatory effect. Specifically, IL-6 levels were significantly reduced by all treatments compared to the CCl_4 group (p < 0.001, Figure 3F), while TNF-α and IL-1β levels also decreased significantly (p < 0.01 for TNF-α and p < 0.001 for IL-1β, Figure 3G,H). These results demonstrate that colchicine and Fx treatments effectively mitigate CCl_4-induced alterations in antioxidant enzymes and inflammatory cytokines, and suppress the inflammatory responses triggered by CCl4 exposure.

3.3. Nrf2, GPX4 Protein Expression in Mouse Kidney. The levels of nuclear factor erythroid 2-related factor 2 (Nrf2) and GPX4 in mouse kidneys were analyzed using immunochemistry (IHC), whereby brown staining indicated positive protein expression. As shown in Figure 4A,B, the results show distinct expression patterns. In the control group, Nrf2 showed high expression in the proximal tubules of the kidneys, whereas its expression was significantly lower in the CCl_4 group (Figure 4A,B). Following colchicine treatment, Nrf2 expression was found to be increased in the glomerulus and tubules, with a significant elevation in the renal tubules post-Fx treatment. GPX4 displayed a similar trend, with elevated expression in the control group's renal tubules and a significant decrease in the CCl_4 group. Colchicine and Fx treatments increased GPX4 levels, particularly in the renal tubules, approximating the expression levels observed in the control group. A semi-quantitative analysis of these proteins corroborated these observations, showing a significant reduction in both Nrf2 and GPX4 in the CCl_4 group. Conversely, the expression of both proteins was significantly restored following drug treatment (p < 0.001, Figure 4C,D). These findings support the protective effects of colchicine and Fx treatments against CCl_4-induced renal damage, emphasizing the important function of Nrf2 and GPX4 in maintaining normal renal health.

3.4. Expression of α-SMA Protein in Mouse Kidney. Compared to the control group, alpha-smooth muscle actin (α-SMA) was significantly elevated in the CCl_4-exposed group (p < 0.05) but significantly reduced by 48%, 42% and 17%in the colchicine (p < 0.001) and L-Fx treatment (p < 0.001) and H-Fx groups (p < 0.05, Figure 5), respectively. These findings highlight the efficacy of colchicine and Fx in mitigating CCl_4-induced kidney injury in mice and the therapeutic potential of colchicine and Fx in alleviating renal injury induced by CCl_4 in mice.

3.5. Nrf2 Pathway Protein Expression in Mouse Kidney. To investigate the molecular mechanism underlying colchicine's amelioration of CCl_4-induced renal injury, we examined the expression levels of Nrf2 pathway-related proteins. Compared to the control group, the CCl_4-exposed

https://doi.org/10.1021/acsomega.4c11437
ACS Omega 2025, 10, 7407−7421

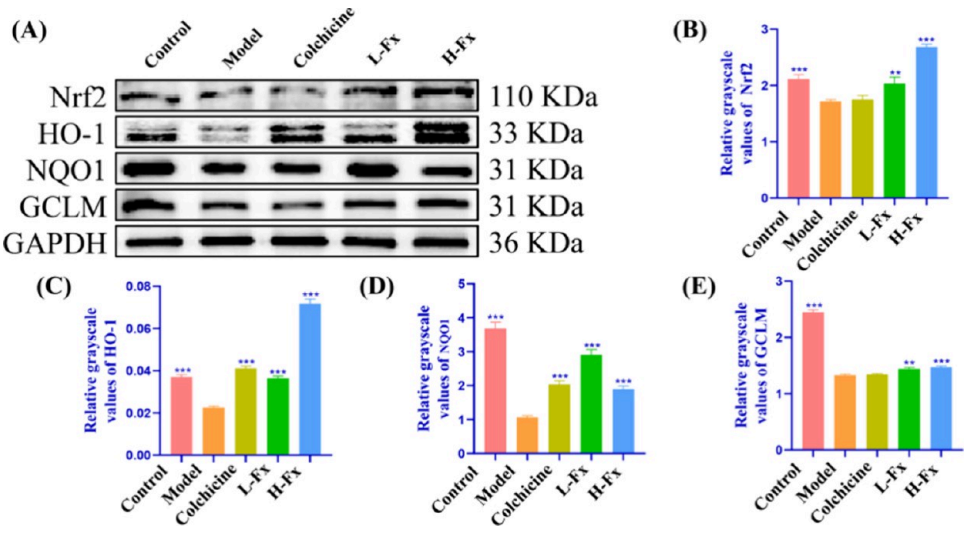

Figure 6. Expression of proteins in the Nrf2 signaling pathway in mice kidneys. (A) Western blot analysis of Nrf2, heme oxygenase-1 (HO-1), nicotinamide quinone oxidoreductase 1 (NQO1) and glutamate-cysteine ligase modifier subunit (GCLM) expression; (B) protein Levels of Nrf2, (C) HO-1, (D) NQO1, and (E) GCLM (n = 3) *p < 0.05, **p < 0.01, *** p < 0.001 vs CCl_4 group.

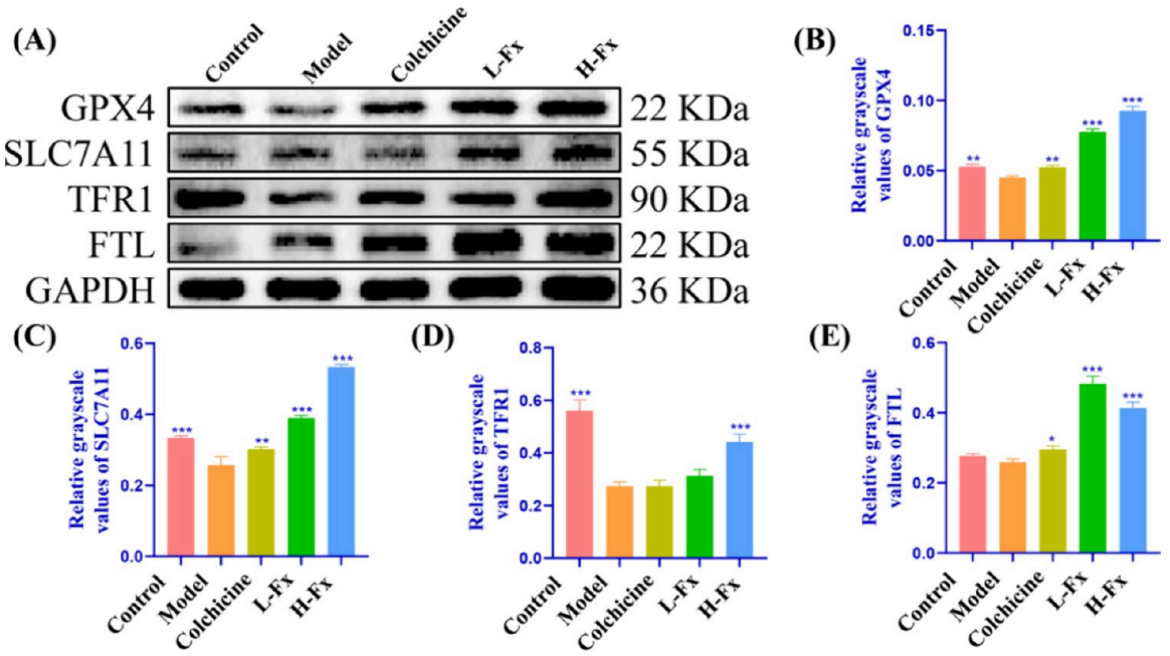

Figure 7. Expression of proteins in the ferroptosis signaling pathway in mouse kidney. (A) Western blot analysis of the expression of GPX4, solute carrier family 7, (cationic amino acid transporter, y+ system) member 11 (SLC7A11), transferrin receptor 1 (TFR1), and ferritin light chain (FTL); (B) Protein levels of GPX4, (C) SLC7A11, (D) TFR1, and (E) FTL (n = 3). *p < 0.05, **p < 0.01, ***p < 0.001 vs CCl_4 group.

group displayed a significant reduction in the levels of Nrf2 and downstream proteins, including heme oxygenase-1 (HO-1), nicotinamide quinone oxidoreductase 1 (NQO1) and glutamate-cysteine ligase modifier subunit (GCLM) (p < 0.001, Figure 6). In contrast, treatment with colchicine and Fx significantly increased these protein levels compared to the CCl_4-exposed group. Specifically, Nrf2 protein levels increased by 18 and 56% in the L-Fx and H-Fx treatment groups, respectively (p < 0.001, Figure 6B). Similarly, HO-1 protein levels increased by 82 and 218% in the colchicine and H-Fx treatment groups, respectively (p < 0.001, Figure 6C). Additionally, NQO1 protein levels increased by 93 and 175% (p < 0.001, Figure 6D), while GCLM protein levels showed respective increases of 1, 9, and 11% in the colchicine, L-Fx, and H-Fx treatment groups (p < 0.001, Figure 6E). These findings suggest that colchicine's protective effects against CCl_4-induced renal injury might be mediated through the modulation of the Nrf2 pathway.

3.6. Expression of Ferroptosis Pathway Proteins in Mouse Kidney. To further elucidate the molecular mechanisms underlying the resolution of CCl_4-induced renal injury by Fx, we assessed the expression of GPX4 pathway-related proteins (Figure 7). The results showed that the GPX4 protein levels were higher in the CCl_4-exposed group than in the control group, and they were further elevated by 16, 73 and 106% in the colchicine, L-Fx and H-Fx treatment groups (p < 0.01, Figure 7B). Additionally, the expression levels of solute carrier family 7, (cationic amino acid transporter, y+ system)

https://doi.org/10.1021/acsomega.4c11437
ACS Omega 2025, 10, 7407−7421

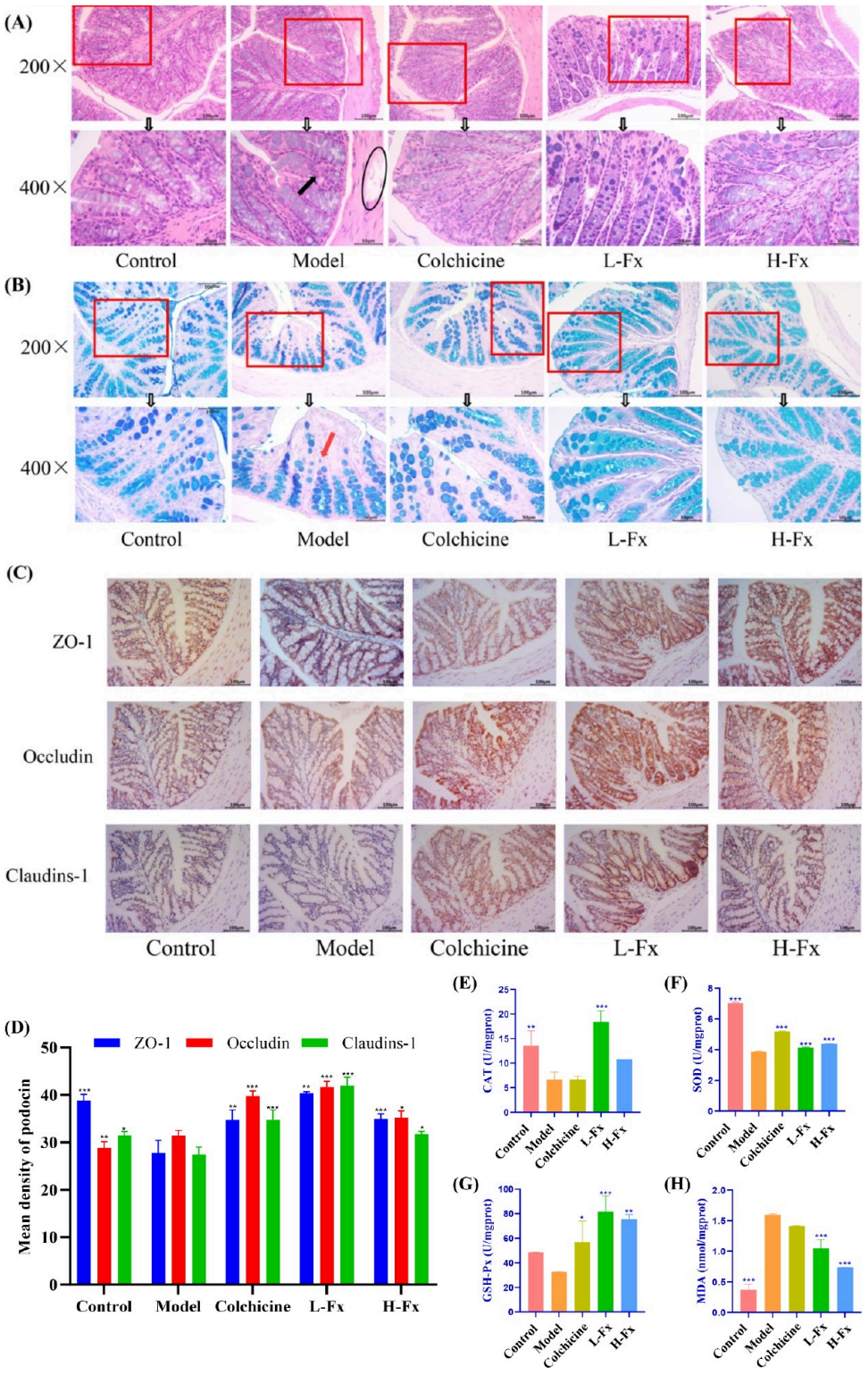

Figure 8. Colon pathological findings and oxidative stress in mice. (A) HE staining and (B) AB-PAS staining of colon tissues (×200, scale bar is 100 μm, upper row; ×400, scale bar is 50 μm, lower row). (C) Expression of zonula occludens-1 (ZO-1), Occludin and Claudins-1 in the colon in mice via IHC (×400, scale bar is 50 μm). (D) ZO-1, Occludin and Claudins-1 protein levels in the colon (n = 3). Levels of (E) CAT, (F) SOD, (G) GSH-Px, (H) MDA in the colon of mice (n = 9). Colonic muscularis propria partially absent (○), inflammatory cells (↑), and areas with fewer cup cells (↑). *p < 0.05, **p < 0.01, ***p < 0.001 vs CCl_4 group.

member 11 (SLC7A11) and transferrin receptor 1 (TFR1) proteins were significantly reduced in the CCl_4-exposed group compared to the control group, with SLC7A11 protein levels increasing by 18, 52 and 107% in the colchicine, L-Fx and H-Fx groups, respectively. TFR1 protein was elevated by 62% in the H-Fx group (p < 0.001, Figure 7C,D). TFR1 protein expression showed no significant difference between the control and CCl_4-exposed groups, while the expression levels

https://doi.org/10.1021/acsomega.4c11437
ACS Omega 2025, 10, 7407−7421

of ferritin light chain (FTL) protein were increased by 14, 87, and 60% in the colchicine, L-Fx, and H-Fx groups, respectively, compared to the CCl_4-exposed group (Figure 7E). These findings provide further insights into the molecular mechanisms underlying the amelioration of CCl_4-induced renal injury by Fx, possibly through the GPX4 pathway.

3.7. Histopathology and Antioxidant Capacity in Mouse Colon. HE and AB-PAS staining techniques were used to assess colonic pathological alterations. In the control group, HE staining revealed an intact mucosal epidermis, whereas the CCl_4-exposed group showed a disrupted epithelial structure, with partial loss of colonic epithelium, fragmented intestinal glands in the lamina propria, and inflammation (Figure 8A). AB-PAS staining further revealed a reduced number of goblet cells in the CCl4-exposed group (blue and green areas), which were significantly increased following Fx treatment (Figure 7B). Biochemical assessment supported these findings, confirming the protective role of the treatments. Intestinal permeability is closely linked to the integrity of tight junction proteins.

IHC revealed a significant reduction in zonula occludens-1 (ZO-1), Claudin-1 and Occludin expressions in the colon of the CCl_4-exposed group compared to the control group. These proteins are key components of tight junctions that maintain the intestinal barrier function, preventing the leakage of harmful substances. ZO-1 helps anchor tight junctions to the actin cytoskeleton, while Claudin-1 and Occludin form the physical seal between adjacent epithelial cells, regulating paracellular permeability. Treatments with colchicine and Fx led to significant upregulation of these proteins, suggesting a restoration of colonic barrier integrity (Figure 8C). Semiquantitative assessment confirmed these findings, revealing a significant upregulation of ZO-1, Claudin-1 and Occludin following treatment with colchicine and Fx (Figure 8D).

Antioxidant enzyme activities were also assessed to further explore the protective role of Fx. CAT activity was significantly reduced in the CCl_4-exposed group (6.67 ± 1.56 U/mgprot) compared to the control group (13.51 ± 3.09 U/mgprot), with substantial restoration observed in the L-Fx group (18.36 ± 2.27 U/mgprot, $p < 0.001$, Figure 8E). SOD levels exhibited similar trends, as it was significantly reduced in the CCl_4-exposed group (3.89 ± 0.03 U/mgprot) and significantly increased after treatments ($p < 0.001$, Figure 8F). Although GSH-Px activity was reduced in the CCl_4-exposed group compared to the control group, this difference was not significant. Comparatively, GSH-Px levels were significantly higher in the colchicine, L-Fx and H-Fx treatment groups compared to the CCl_4-exposed group ($p < 0.05$, Figure 8G).

MDA levels were elevated in the CCl_4-exposed group and subsequently reduced in the L-Fx and H-Fx treatment groups to 66 and 46%, respectively ($p < 0.001$, Figure 8H). These results further support the protective effects of Fx on both oxidative stress and colonic integrity. Overall, these observations highlight the potential therapeutic utility of colchicine and Fx in mitigating CCl_4-induced colonic damage, offering valuable insights into their mechanisms of action and contributing to our understanding of intestinal protection.

3.8. Histopathology, Antioxidant and Proinflammatory Cytokines in the Jejunum. Histological examination of jejunal tissues revealed significant differences in morphology and biochemical parameters among various experimental groups. In the jejunal HE staining, the control group exhibited neatly arranged jejunal villi, while the CCl_4-exposed group demonstrated a noticeable loss of intestinal villi, reduction in villi height, and increased crypt depth. Interestingly, treatments with colchicine and Fx ameliorated these alterations (Figure 9A). IHC was also performed to detect tight junction proteins,

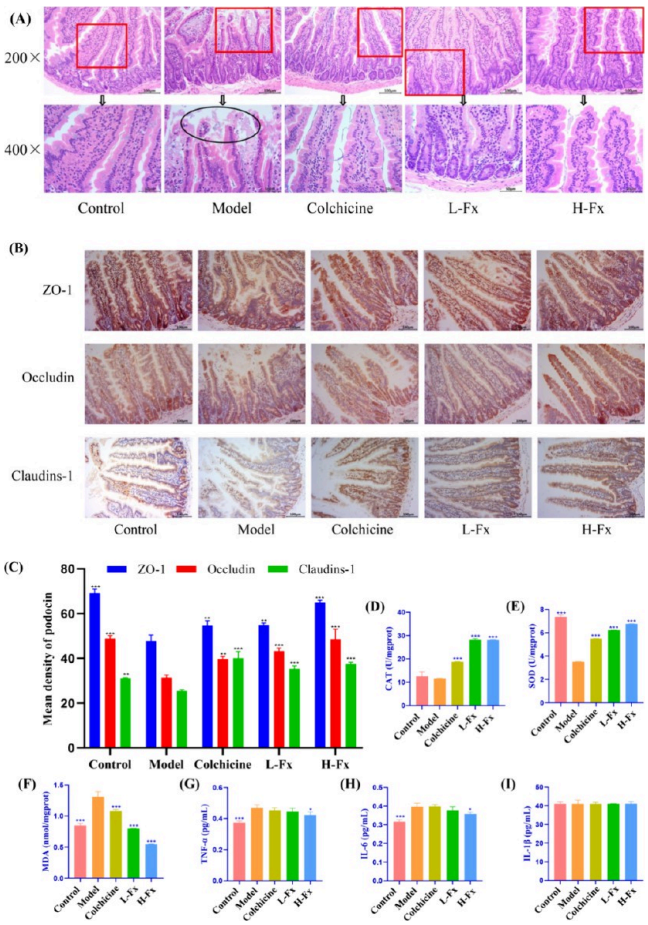

Figure 9. Jejunum pathological findings, oxidative stress and inflammation in mice. (A) HE staining of jejunum tissues (×200, scale bar is 100 μm, ×400, scale bar is 50 μm). (B) Expression of ZO-1, Occludin and Claudins-1 proteins in the jejunum of mice via IHC (×400, scale bar is 50 μm). (C) ZO-1, Occludin and Claudins-1 protein levels in the jejunum ($n = 3$). Levels of (D) CAT, (E) SOD, (F) MDA ($n = 9$); (G) TFN-α, (H) IL-6, (I) IL-1β in the jejunum of mice ($n = 3$). Jejunal villi shedding (○). *$p < 0.05$, **$p < 0.01$, ***$p < 0.001$ vs CCl_4 group.

such as ZO-1, Occludin and Claudin-1, in the jejunum. Compared to the control group, the CCl_4-exposed group exhibited a significant reduction in the expression of these proteins in the jejunum tissues. However, treatments with colchicine or Fx effectively restored their expression levels (Figure 9B). Semiquantitative analysis supported these findings, indicating that colchicine and Fx improve the structure and barrier function of the jejunum (Figure 9C).

A comprehensive biochemical assessment was conducted to evaluate the antioxidant levels and inflammatory markers within the jejunal tissue. Compared to the control group, the CCl_4-exposed group showed a nonsignificant reduction in CAT activity ($p > 0.05$, Figure 9D), a significant decrease in SOD activity ($p < 0.001$, Figure 9E), and a significant increase in MDA, TNF-α, and IL-6 levels ($p < 0.05$, Figure 9F−H). In contrast to the CCl_4 group, CAT activity was significantly

https://doi.org/10.1021/acsomega.4c11437
ACS Omega 2025, 10, 7407−7421

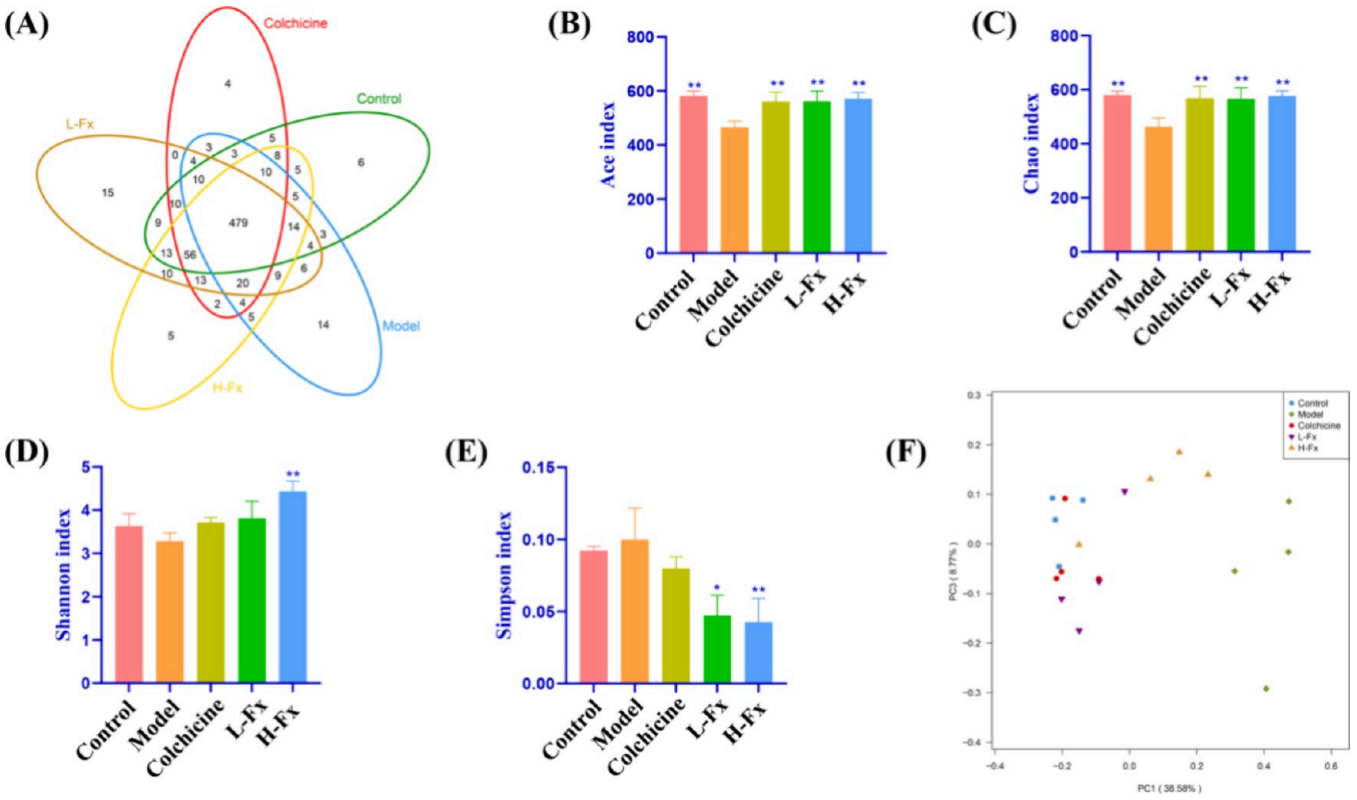

Figure 10. Sequencing statistics and Alpha/Beta-diversity analysis of mouse intestinal microbiota. (A) Venn diagram, (B) Ace index, (C) Chao index, (D) Shannon index, (E) Simpson index, and (F) Principal coordinates analysis (PCOA) (n = 4). *p < 0.05, **p < 0.01, ***p < 0.001 vs CCl_4 group.

increased to 162, 244, and 243% in the colchicine, L-Fx, and H-Fx groups, respectively (p < 0.001, Figure 9D), along with a significant elevation in SOD activity (156, 177, and 192%, respectively; p < 0.001, Figure 9E). Conversely, MDA activity decreased to 82, 61, and 42% in the colchicine, L-Fx, and H-Fx groups, respectively (p < 0.001, Figure 9F). TNF-α and IL-6 levels were significantly lower in the H-Fx group (p < 0.05, Figure 9G,H). Interestingly, the levels of IL-1β remained unchanged across the different experimental groups (p > 0.05, Figure 9I). These findings collectively demonstrate the therapeutic potential of colchicine and Fx in mitigating CCl_4-induced jejunal injury, possibly through the modulation of antioxidant and inflammatory pathways, offering valuable insights into strategies for addressing gastrointestinal disturbances.

3.9. Sequencing Statistics and Alpha/Beta Diversity Analysis of Mouse Intestinal Flora. Next, we assessed the impact of Fx on the intestinal microbiota through 16S rRNA gene sequencing to determine the composition and diversity of microbial communities in fecal samples. Venn diagrams were drawn to illustrate the quantity of common Operational taxonomic units (OTUs) among different samples and groups (Figure 10A). Across all samples, we identified 479 OTUs, with a 70% overlap of OTUs observed between the CCl_4-exposed group and the control, indicating that the CCl_4 group had a 30% different intestinal flora composition compared to the control group. The overlapping OTUs between the control and colchicine, L-Fx, and H-Fx groups were 77, 78, and 78%, respectively, suggesting a closer resemblance in microbial composition to the control.

Alpha diversity analyses revealed significant alterations in the Ace and Chao indices for the CCl_4-induced mice compared to the control group, indicating a decrease in diversity that was subsequently restored in the colchicine, L-Fx, and H-Fx groups (p < 0.01, Figure 10B,C). Although the Shannon index exhibited a nonsignificant decrease in the CCl_4 group compared to the control group, it displayed a significant increase in the H-Fx group (p < 0.01, Figure 10D). Similarly, the Simpson index (Figure 10E) was elevated in the CCl_4 group relative to the control group but showed a significant reduction in all treatment groups (p < 0.05). These data collectively suggest that Fx effectively modulates the composition and diversity of the intestinal microbiota, promoting a microbial environment more similar to that of the control group.

PCoA was conducted to assess similarities and differences among multiple samples (Figure 10F). The separation of the CCl_4 group from the other categories in the figure highlights distinct microbial community compositions, indicating significant differences compared to the other groups. Specifically, the CCl_4-induced alterations in the mouse microbiota showed a significant deviation from the control group, but this shift was partially mitigated, especially in the colchicine and L-Fx-treated groups. These results indicate the profound impact of CCl_4 on intestinal flora and the potential corrective influence of both Fx and colchicine treatments.

3.10. Analysis of Community Differences in the Intestinal Flora of Mice. At the phylum level, *Firmicutes* and *Bacteroidetes* were identified as the dominant gut microbiota phyla. The *Firmicutes*/*Bacteroidetes* (F/B) ratio increased in the CCl_4 group compared to the control group,

https://doi.org/10.1021/acsomega.4c11437
ACS Omega 2025, 10, 7407−7421

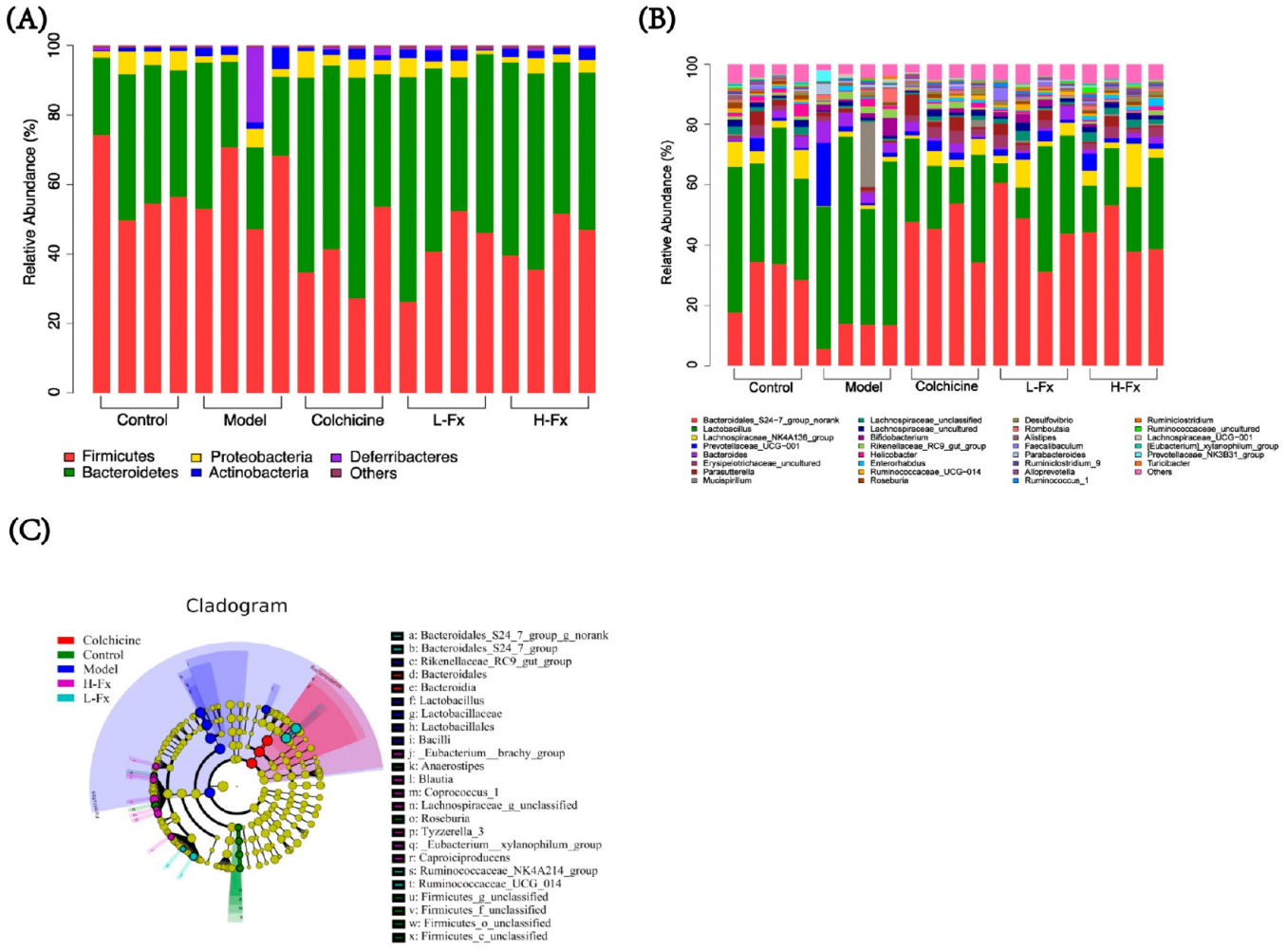

Figure 11. Composition of the gut microbiota of mice examined at (A) phylum levels, (B) genus levels, and (C) via LEFSE analysis (n = 4).

indicating a shift in microbial composition. Additionally, the proinflammatory phylum *Desferobacteria* showed an increase in the CCl_4 group. Interestingly, these alterations in the F/B ratio were reversed after the administration of colchicine and Fx (Figure 11A). At the genus level, *Bacteroidales* and *Lachnospiraceae* were increased after administration of colchicine and Fx, while *Lactobacillus* were decreased (Figure 11B).

The results of Linear Discriminant Analysis Effect Size (LEfSe) analysis provided further insight into the microbial changes. Compared to the CCl_4 group, Fx was found to decrease the relative abundance of *Rikeniaceae-RC9 group*, *Bacillus* and *Lactobacillus* and increased the relative abundance of *Brault's* and *Lactobacillus acidophilus* (Figure 11C). These findings collectively demonstrate the intricate interplay between CCl_4-induced alterations and subsequent treatment with colchicine and Fx and their potential therapeutic roles in modulating gut microbiota composition.

3.11. Analysis of the Correlation Between Intestinal Flora and Some Biological Indicators in the Kidney and Serum. Here, we systematically explored the complex interactions between intestinal flora and renal fibrosis (Figure 12). A network of associations illustrates the multifaceted connections between gut microbiota and renal markers, indicating that *Turicibacter* was positively correlated with MDA and α-SMA, while *Candidatus* was negatively correlated with these markers. *Parabacteroides* and *Bacteroides* were negatively correlated with Nrf2 and SLC7A11 but positively correlated with TNF-α and IL-6. In addition, *Tyzzerella*, *Lachnospiracea* and *Eubacterium* were positively correlated with Nrf2 and SLC7A11, *Lachnospiraceae*, *Eubacterium*, *Ruminococcaceae* and *Coprococcus* were negatively correlated with IL-6 and TNF-α, and *Coprococcus*, *Blautia* and *Ruminococchaceae* were positively correlated with SLC7A11. Various microbial taxa, including *Coriobacteriaceae*, *Bacteroidales*, *Erysipelotrichaceae*, *Faecalibaculum* and *Gastranaerophilales*, were negatively correlated with MDA, α-SMA and IL-1β. A subset of bacteria exhibited unique correlations; for instance, *Ricardiaceae* was linked with SLC7A11, *Anaerostipes caccae* with IL-6, and *Ruminococcaceae* was negatively correlated with GSH Px. Furthermore, *Lactobacillus* was correlated with IL-1β, *Peptococaceae* with GPX4, and *Bifidobacterium* was positively correlated with BUN. These findings shed light on the complex network of interactions between the gut microbiota and renal fibrosis, suggesting potential pathways through which these specific bacterial taxa may influence renal function. Understanding these relationships provides valuable insights into potential therapeutic strategies for mitigating renal fibrosis and underscores the integrative nature of host-microbiome interactions.

https://doi.org/10.1021/acsomega.4c11437
ACS Omega 2025, 10, 7407−7421

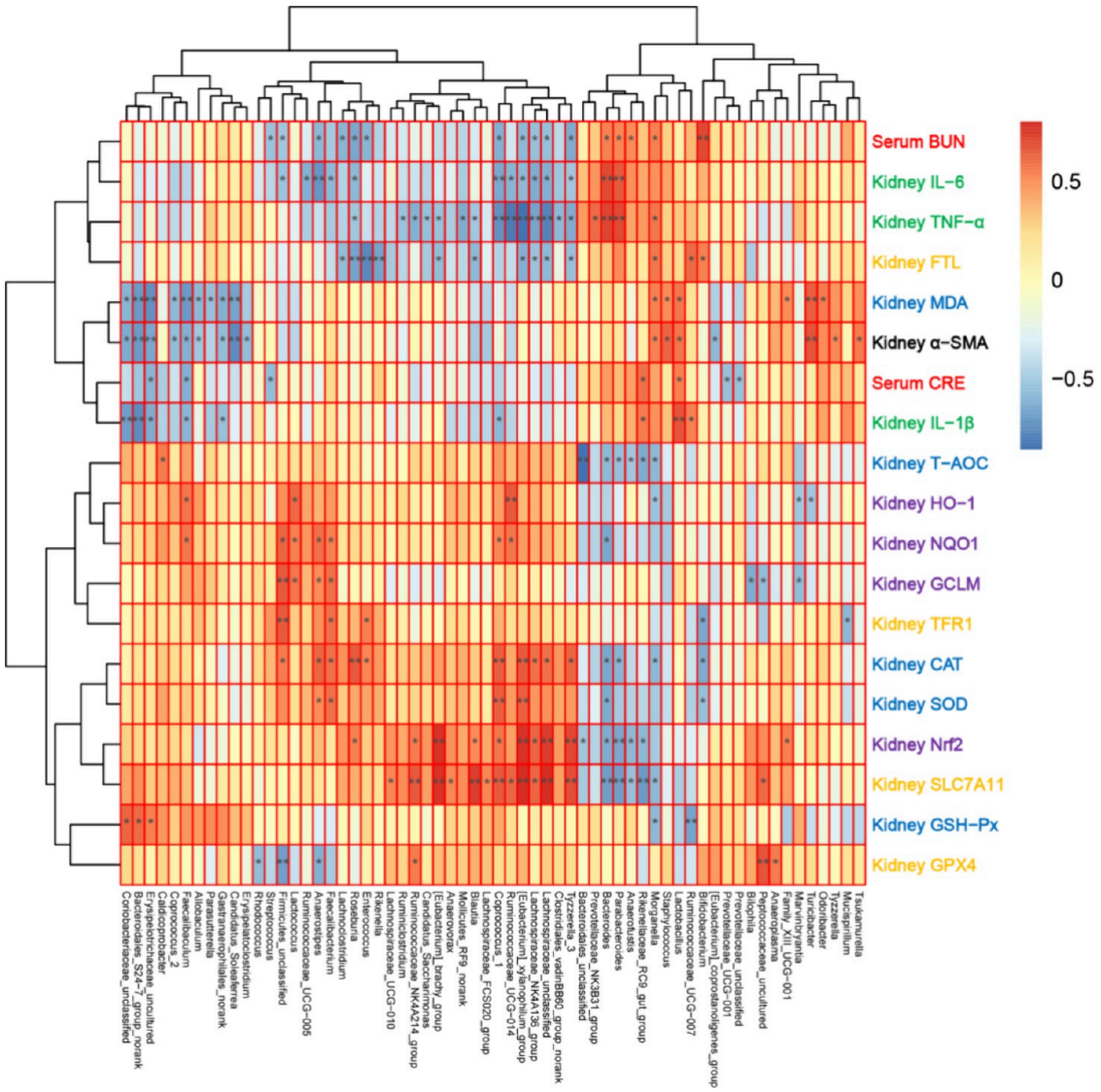

Figure 12. Heatmap of Pearson Correlation Analysis Between Intestinal Flora and the Traits of Kidney Damage.

4. DISCUSSION

CCl_4 is a known hepatotoxic and nephrotoxic agent that induces oxidative stress, inflammation, and renal injury through the excessive generation of reactive oxygen species (ROS). In this study, Fx demonstrated significant protective effects against CCl_4-induced renal injury by mitigating oxidative stress, enhancing antioxidant enzyme activities, and reducing inflammatory cytokine levels, which highlights its potential as a therapeutic agent for oxidative stress-related kidney disorders.

Previous research has shown that Fx can ameliorate renal fibrosis, particularly through the upregulation of NHE11 and the Akt/Sirt1/FoxO3α signaling pathway,[30,31] and its ability to prevent hyperuricemia[32]and oxidative stress.[33] The assessment of renal function often relies on the measurement of serum CRE and BUN levels, with variations in these markers indicative of varying degrees of renal injury.[34−36] In this study, we observed significant improvements in serum markers of renal function, such as CRE and BUN, as well as a reduction in α-SMA expression, a marker of fibrosis. Histopathological analysis further confirmed the protective effects of Fx on kidney structure, supporting its role in restoring renal function in CCl_4-induced injury.

Oxidative stress plays a crucial role in various renal injuries, such as disrupting innate redox homeostasis and exacerbating tissue oxidative damage.[37,38] Fx effectively reduced MDA levels and enhanced the activities of key antioxidant enzymes, including GSH-Px, CAT, and SOD, thereby counteracting the oxidative damage induced by CCl_4. These effects were mediated by Nrf2, a transcriptional regulator that upregulates protective proteins such as HO-1 to combat oxidative damage.[39,40] Additionally, the treatment with Fx resulted in the restoration of depleted GSH and GPX4 levels, which are critical in reducing ROS production and inflammation.[41] In addition to its antioxidant effects, Fx also demonstrated anti-inflammatory properties by significantly reducing the expression of proinflammatory cytokines such as IL-6, TNF-α, and IL-1β, which are elevated in CCl_4-induced kidney injury.[42] These cytokines contribute to renal damage by promoting inflammation and fibrosis, and their reduction further underscores the therapeutic potential of Fx in kidney diseases characterized by inflammation and oxidative stress.

https://doi.org/10.1021/acsomega.4c11437
ACS Omega 2025, 10, 7407−7421

Ferroptosis, initially characterized in 2012, is a distinct form of programmed cell death marked by the decline of GPX4 activity and accumulation of lipid hydroperoxides.[43,44] Mice with lung fibrosis have decreased GPX4 expression, and the fibrosis is more severe when GPX4 is knocked out.[45] Recent studies have shown that almost all genes associated with ferroptosis are transcriptionally regulated by Nrf2[46], which regulates ferroptosis through the Nrf2/HO-1 axis.[46,47] Activation of this axis has been shown to deter ferroptosis, thereby facilitating organ function restoration.[48]

It was shown that GPX4 expression was negatively correlated with tubular injury and positively correlated with renal function in cisplatin-stimulated mice.[49] In addition to ferroptosis, which is closely associated with a decrease in GPX4, TFR1 also affects renal iron cycling and systemic iron homeostasis, and acute renal injury due to TFR1 deficiency in the proximal tubule was found to attenuate ferroptosis by upregulating ferritin heavy chain (FTH1) expression.[50] Our results show that Fx alleviated CCl_4-induced renal injury by modulating ferroptosis-related proteins, including GPX4, SLC7A11, TFR1, and FTL. By activating the Nrf2/HO-1 axis, Fx suppressed ferroptosis and improved renal function, reinforcing its potential to target ferroptosis as a therapeutic strategy for kidney injuries.

Intestinal microbiota dysbiosis has been increasingly recognized as a key factor in the pathogenesis of various diseases,[51] including kidney injury.[52] Disruption of the intestinal barrier, often seen in such dysbiosis, leads to the translocation of bacterial endotoxins into the circulatory system, triggering systemic inflammation and oxidative stress.[53,54] This process contributes to kidney damage and is often associated with altered microbiota composition.In this study, we demonstrate that treatment with 50 mg/kg Fx significantly alleviates CCl_4-induced kidney injury, likely by repairing the intestinal barrier and modulating gut microbiota composition.[55,56]

Our results show that CCl_4 exposure impairs intestinal barrier function, as evidenced by a reduction in tight junction protein expression in both the colon and jejunum. This disruption was largely reversed by Fx treatment, which restored intestinal permeability and improved gut epithelial integrity. Furthermore, histological analysis revealed that Fx treatment enhanced the number of goblet cells and mucin secretion, reinforcing the intestinal mucus layer, thus providing a protective barrier against pathogenic invasion. These findings suggest that Fx may help restore the intestinal barrier, thereby ameliorating kidney injury by mitigating the harmful effects of endotoxins and other bacterial metabolites.

Alterations in the gut microbiota composition are closely linked to changes in intestinal permeability. 16S rRNA gene sequencing revealed that Fx treatment reduced the relative abundance of *Bacilli* while promoting an increase in *Bacteroides*, *Clostridia*, and *Erysipelotrichia*, thus favoring a more balanced and potentially protective microbial community. Notably, the *Firmicutes*/*Bacteroidetes* (F/B) ratio, an established marker of dysbiosis, was significantly reduced in the Fx-treated group, underscoring the regulatory effect of Fx on gut microbiota composition.

Further, we observed changes in specific taxa with potential implications for kidney health.[58] The *Lachnospiraceae* family, known for its role in maintaining intestinal barrier integrity,[57] was modulated by Fx treatment. While *Lactobacilli* have traditionally been considered beneficial for preventing inflammation, recent studies suggest their involvement in a range of diseases.[26,59] Our study found an increased abundance of *Lactobacillus* in the CCl_4 group, which was subsequently reduced by Fx treatment, warranting further investigation into the role of these taxa in renal pathology. Similarly, *Prevotella*, a genus linked to increased intestinal permeability and inflammation,[60] was also altered in response to Fx, suggesting its potential role in the gut-kidney axis.

The relationship between the intestinal microbiota and kidney injury is complex and bidirectional.[61] Recent studies have highlighted the potential of microbiota modulation as a therapeutic approach for kidney disease.[62] Our Pearson correlation analysis revealed a significant association between microbiota composition and markers of renal injury, inflammation, and key proteins in the Nrf2 and GPX4 pathways. This suggests that gut microbiota composition may influence kidney health by modulating oxidative stress and inflammatory responses, emphasizing the potential therapeutic benefits of targeting the microbiota in renal disease.

Our findings contribute to the growing body of evidence supporting the gut-kidney axis as a critical pathway in kidney disease. The regulation of intestinal microbiota by Fx represents a novel strategy for mitigating CCl_4-induced kidney injury, potentially through the repair of intestinal permeability and the modulation of microbial-derived metabolites. However, further studies, including the use of GPX4-deficient mice and more extensive exploration of iron metabolism, are needed to fully elucidate the mechanisms underlying these effects.

In conclusion, our study underscores the importance of gut microbiota in the pathogenesis of kidney injury and highlights Fx as a promising therapeutic agent that may repair the intestinal barrier, restore microbial balance, and protect against kidney damage. Future research should focus on identifying the specific microbial taxa and metabolites involved in these processes and explore potential interventions that leverage the gut-kidney axis for the prevention and treatment of renal diseases.

5. CONCLUSIONS

In conclusion, our study demonstrates that Fx treatment effectively modulates both the Nrf2 and ferroptosis signaling pathways, thereby mitigating renal injury in CCl_4-induced ICR mice. Additionally, Fx positively influences the composition of the gut microbiota, further contributing to renal injury alleviation. These findings not only highlight the intricate interplay between renal function and gut health but also support Fx as a promising therapeutic candidate for addressing kidney injury. These insights offer potential for innovative strategies in managing renal disorders and warrant further exploration and validation in clinical settings.

■ ASSOCIATED CONTENT

Data Availability Statement

The data is available throughout the manuscript

■ AUTHOR INFORMATION

Corresponding Authors

Zuisu Yang − *School of Food and Pharmacy, Zhejiang Ocean University, Zhoushan 316022, China;* orcid.org/0000-0002-4290-197X; Email: yzs@zjou.edu.cn

Zhongliang Liu − *Zhoushan Hospital of Traditional Chinese Medicine Affiliated to Zhejiang Chinese Medical University,*

https://doi.org/10.1021/acsomega.4c11437
ACS Omega 2025, 10, 7407−7421

Zhoushan 316000 Zhejiang Province, P.R. China; Email: 2021a001@zcmu.edu.cn

Authors

Yaping Ding − *Zhoushan Hospital of Traditional Chinese Medicine Affiliated to Zhejiang Chinese Medical University, Zhoushan 316000 Zhejiang Province, P.R. China*

Jiena Ye − *School of Food and Pharmacy, Zhejiang Ocean University, Zhoushan 316022, China*

Ying Liu − *Zhoushan Hospital of Traditional Chinese Medicine Affiliated to Zhejiang Chinese Medical University, Zhoushan 316000 Zhejiang Province, P.R. China*

Shaohua Zhang − *Zhoushan Hospital of Traditional Chinese Medicine Affiliated to Zhejiang Chinese Medical University, Zhoushan 316000 Zhejiang Province, P.R. China*

Yan Xu − *Zhoushan Hospital of Traditional Chinese Medicine Affiliated to Zhejiang Chinese Medical University, Zhoushan 316000 Zhejiang Province, P.R. China*

Complete contact information is available at: https://pubs.acs.org/10.1021/acsomega.4c11437

Author Contributions

Conceptualization, Y.L., S.W., S.Z. and Y.X.; methodology, Y.D., J.Y., Y.L., S.W., S.Z. and Y.X.; software, J.Y.; validation, Y.L., S.W., S.Z. and Y.X.; formal analysis, Z.Y., Z.L., Y.D. and J.Y.; investigation, Z.Y., Z.L., Y.D. and J.Y.; resources, Y.D.; data curation, J.Y.; writing—original draft preparation, Y.D. and J.Y.; writing—review and editing, Y.L., S.W., S.Z. and Y.X.; visualization, Y.L., S.W., S.Z. and Y.X.; supervision, Y.L., S.W., S.Z. and Y.X.; project administration, Y.L., S.W., S.Z. and Y.X.; funding acquisition, Y.Y. All authors have read and agreed to the published version of the manuscript. Y.D. and J.Y. are contributed equally to this work.

Funding

This research was funded by Zhejiang Provincial Medical and Health Technology Plan Project, grant numbers 2023RC109 and 2024kY1776 and Zhoushan Municipal Public Welfare Technology Projects, grant numbers 2022C31021 and 2023C31021.

Notes

The authors declare no competing financial interest.

The Experimental Animal Ethics Committee of Zhejiang Ocean University approved the procedures for the use of laboratory animals (2020028, approval date: October 10, 2020).

■ ACKNOWLEDGMENTS

Not applicable.

■ REFERENCES

(1) Lameire, N. H.; Levin, A.; Kellum, J. A.; Cheung, M.; Jadoul, M.; Winkelmayer, W. C.; Stevens, P. E. Harmonizing acute and chronic kidney disease definition and classification: report of a Kidney Disease: Improving Global Outcomes (KDIGO) Consensus Conference. *Kidney Int.* **2021**, *100* (3), 516−526.

(2) Giordano, L.; Mihaila, S. M.; Eslami Amirabadi, H.; Masereeuw, R. Microphysiological Systems to Recapitulate the Gut-Kidney Axis. *Trends Biotechnol* **2021**, *39* (8), 811−823.

(3) Cao, C.; Zhu, H.; Yao, Y.; Zeng, R. Gut Dysbiosis and Kidney Diseases. *Front Med. (Lausanne)* **2022**, *9*, No. 829349.

(4) Dafa, D.; Yibing, L. U.; Tingting, C. A. I.; Xiaolong, Y. E.; Jianhua, M. A. O. 27-LB: Alteration of the Gut Microbiome by Resveratrol Is Associated with Improvement in Function of Kidney in db/db Mice. *Diabetes* **2019**, *68*, 27-LB.

(5) Hsu, C. N.; Hou, C. Y.; Chang, C. I.; Tain, Y. L. Resveratrol Butyrate Ester Protects Adenine-Treated Rats against Hypertension and Kidney Disease by Regulating the Gut-Kidney Axis. *Antioxidants (Basel)* **2022**, *11* (1), 83.

(6) Hua, Q.; Han, Y.; Zhao, H.; Zhang, H.; Yan, B.; Pei, S.; He, X.; Li, Y.; Meng, X.; Chen, L.; Zhong, F.; Li, D. Punicalagin alleviates renal injury via the gut-kidney axis in high-fat diet-induced diabetic mice. *Food Funct* **2022**, *13* (2), 867−879.

(7) Qi, J.; Kim, J. W.; Zhou, Z.; Lim, C. W.; Kim, B. Ferroptosis Affects the Progression of Nonalcoholic Steatohepatitis via the Modulation of Lipid Peroxidation-Mediated Cell Death in Mice. *Am. J. Pathol.* **2020**, *190* (1), 68−81.

(8) Wang, Y.; Peng, X.; Zhang, M.; Jia, Y.; Yu, B.; Tian, J. Revisiting Tumors and the Cardiovascular System: Mechanistic Intersections and Divergences in Ferroptosis. *Oxid. Med. Cell. Longevity* **2020**, *2020*, No. 9738143.

(9) Zhang, Y.; Mou, Y.; Zhang, J.; Suo, C.; Zhou, H.; Gu, M.; Wang, Z.; Tan, R. Therapeutic Implications of Ferroptosis in Renal Fibrosis. *Front Mol. Biosci* **2022**, *9*, No. 890766.

(10) Zhang, J.; Wang, B.; Yuan, S.; He, Q.; Jin, J. The Role of Ferroptosis in Acute Kidney Injury. *Front Mol. Biosci* **2022**, *9*, No. 951275.

(11) Ni, L.; Yuan, C.; Wu, X. Targeting ferroptosis in acute kidney injury. *Cell Death Dis.* **2022**, *13* (2), 182.

(12) Wang, J.; Wang, Y.; Liu, Y.; Cai, X.; Huang, X.; Fu, W.; Wang, L.; Qiu, L.; Li, J.; Sun, L. Ferroptosis, a new target for treatment of renal injury and fibrosis in a 5/6 nephrectomy-induced CKD rat model. *Cell Death Discovery* **2022**, *8* (1), 127.

(13) Wang, J.; Liu, Y.; Wang, Y.; Sun, L. The Cross-Link between Ferroptosis and Kidney Diseases. *Oxid. Med. Cell. Longevity* **2021**, *2021*, No. 6654887.

(14) Liu, Y.; Wang, J.; Badr, D. A. Ferroptosis, a Rising Force against Renal Fibrosis. *Oxid. Med. Cell. Longevity* **2022**, *2022*, No. 7686956.

(15) Wang, Y.; Quan, F.; Cao, Q.; Lin, Y.; Yue, C.; Bi, R.; Cui, X.; Yang, H.; Yang, Y.; Birnbaumer, L.; Li, X.; Gao, X. Quercetin alleviates acute kidney injury by inhibiting ferroptosis. *J. Adv. Res.* **2021**, *28*, 231−243.

(16) Zhou, L.; Yu, P.; Wang, T. T.; Du, Y. W.; Chen, Y.; Li, Z.; He, M. L.; Feng, L.; Li, H. R.; Han, X.; Ma, H.; Liu, H. B. Polydatin Attenuates Cisplatin-Induced Acute Kidney Injury by Inhibiting Ferroptosis. *Oxid. Med. Cell. Longevity* **2022**, *2022*, No. 9947191.

(17) Zhang, B.; Chen, X.; Ru, F.; Gan, Y.; Li, B.; Xia, W.; Dai, G.; He, Y.; Chen, Z. Liproxstatin-1 attenuates unilateral ureteral obstruction-induced renal fibrosis by inhibiting renal tubular epithelial cells ferroptosis. *Cell Death Dis.* **2021**, *12* (9), 843.

(18) Lo, Y. H.; Yang, S. F.; Cheng, C. C.; Hsu, K. C.; Chen, Y. S.; Chen, Y. Y.; Wang, C. W.; Guan, S. S.; Wu, C. T. Nobiletin Alleviates Ferroptosis-Associated Renal Injury, Inflammation, and Fibrosis in a Unilateral Ureteral Obstruction Mouse Model. *Biomedicines* **2022**, *10* (3), 595.

(19) Qiu, W.; An, S.; Wang, T.; Li, J.; Yu, B.; Zeng, Z.; Chen, Z.; Lin, B.; Lin, X.; Gao, Y. Melatonin suppresses ferroptosis via activation of the Nrf2/HO-1 signaling pathway in the mouse model of sepsis-induced acute kidney injury. *Int. Immunopharmacol* **2022**, *112*, No. 109162.

(20) Xu, B.; Zheng, J.; Tian, X.; Yuan, F.; Liu, Z.; Zhou, Y.; Yang, Z.; Ding, X. Protective mechanism of traditional Chinese medicine guizhi fuling pills against carbon tetrachloride-induced kidney damage is through inhibiting oxidative stress, inflammation and regulating the intestinal flora. *Phytomedicine* **2022**, *101*, No. 154129.

(21) Karpiński, T. M.; Ożarowski, M.; Alam, R.; Łochyńska, M.; Stasiewicz, M. What Do We Know about Antimicrobial Activity of Astaxanthin and Fucoxanthin? *Mar Drugs* **2022**, *20* (1), 36.

(22) Yang, H.; Xing, R.; Liu, S.; Yu, H.; Li, P. Role of Fucoxanthin towards Cadmium-induced renal impairment with the antioxidant and anti-lipid peroxide activities. *Bioengineered* **2021**, *12* (1), 7235−7247.

(23) Yang, G.; Jin, L.; Zheng, D.; Tang, X.; Yang, J.; Fan, L.; Xie, X. Fucoxanthin Alleviates Oxidative Stress through Akt/Sirt1/FoxO3α Signaling to Inhibit HG-Induced Renal Fibrosis in GMCs. *Mar Drugs* **2019**, *17* (12), 702.
(24) Yang, G.; Li, Q.; Peng, J.; Jin, L.; Zhu, X.; Zheng, D.; Zhang, Y.; Wang, R.; Song, Y.; Hu, W.; Xie, X. Fucoxanthin regulates Nrf2 signaling to decrease oxidative stress and improves renal fibrosis depending on Sirt1 in HG-induced GMCs and STZ-induced diabetic rats. *Eur. J. Pharmacol.* **2021**, *913*, No. 174629.
(25) Han, B.; Ma, Y.; Liu, Y. Fucoxanthin Prevents the Ovalbumin-Induced Food Allergic Response by Enhancing the Intestinal Epithelial Barrier and Regulating the Intestinal Flora. *J. Agric. Food Chem.* **2022**, *70* (33), 10229−10238.
(26) Xu, B.; Zheng, J.; Tian, X.; Yuan, F.; Liu, Z.; Zhou, Y.; Yang, Z.; Ding, X. Protective mechanism of traditional Chinese medicine guizhi fuling pills against carbon tetrachloride-induced kidney damage is through inhibiting oxidative stress, inflammation and regulating the intestinal flora. *Phytomedicine* **2022**, *101*, No. 154129.
(27) Long, T.; Wang, L.; Yang, Y.; Yuan, L.; Zhao, H.; Chang, C. C.; Yang, G.; Ho, C. T.; Li, S. Protective effects of trans-2,3,5,4'-tetrahydroxystilbene 2-O-β-d-glucopyranoside on liver fibrosis and renal injury induced by CCl(4)via down-regulating p-ERK1/2 and p-Smad1/2. *Food Funct* **2019**, *10* (8), 5115−5123.
(28) Wang, C.; Ma, C.; Fu, K.; Gong, L. H.; Zhang, Y. F.; Zhou, H. L.; Li, Y. X. Phillygenin Attenuates Carbon Tetrachloride-Induced Liver Fibrosis via Modulating Inflammation and Gut Microbiota. *Front Pharmacol* **2021**, *12*, No. 756924.
(29) Liu, J.; Fu, Y.; Zhang, H.; Wang, J.; Zhu, J.; Wang, Y.; Guo, Y.; Wang, G.; Xu, T.; Chu, M.; Wang, F. The hepatoprotective effect of the probiotic Clostridium butyricum against carbon tetrachloride-induced acute liver damage in mice. *Food Funct* **2017**, *8* (11), 4042−4052.
(30) Chen, Y. C.; Cheng, C. Y.; Liu, C. T.; Sue, Y. M.; Chen, T. H.; Hsu, Y. H.; Hwang, P. A.; Chen, C. H. Alleviative effect of fucoxanthin-containing extract from brown seaweed Laminaria japonica on renal tubular cell apoptosis through upregulating Na(+)/H(+) exchanger NHE1 in chronic kidney disease mice. *J. Ethnopharmacol* **2018**, *224*, 391−399.
(31) Chang, Y. H.; Chen, Y. L.; Huang, W. C.; Liou, C. J. Fucoxanthin attenuates fatty acid-induced lipid accumulation in FL83B hepatocytes through regulated Sirt1/AMPK signaling pathway. *Biochem. Biophys. Res. Commun.* **2018**, *495* (1), 197−203.
(32) Chau, Y. T.; Chen, H. Y.; Lin, P. H.; Hsia, S. M. Preventive Effects of Fucoidan and Fucoxanthin on Hyperuricemic Rats Induced by Potassium Oxonate. *Mar Drugs* **2019**, *17* (6), 343.
(33) Mao, H.; Wang, L.; Xiong, Y.; Jiang, G.; Liu, X. Fucoxanthin Attenuates Oxidative Damage by Activating the Sirt1/Nrf2/HO-1 Signaling Pathway to Protect the Kidney from Ischemia-Reperfusion Injury. *Oxid. Med. Cell. Longevity* **2022**, *2022*, No. 7444430.
(34) Chen, J.; Xu, L.; Jiang, L.; Wu, Y.; Wei, L.; Wu, X.; Xiao, S.; Liu, Y.; Gao, C.; Cai, J.; Su, Z. Sonneratia apetala seed oil attenuates potassium oxonate/hypoxanthine-induced hyperuricemia and renal injury in mice. *Food Funct* **2021**, *12* (19), 9416−9431.
(35) Li, L.; Li, Y.; Luo, J.; Jiang, Y.; Zhao, Z.; Chen, Y.; Huang, Q.; Zhang, L.; Wu, T.; Pang, J. Resveratrol, a novel inhibitor of GLUT9, ameliorates liver and kidney injuries in a D-galactose-induced ageing mouse model via the regulation of uric acid metabolism. *Food Funct* **2021**, *12* (18), 8274−8287.
(36) Bai, H.; Zhang, Z.; Ma, X.; Shen, M.; Li, R.; Li, S.; Qiu, D.; Gao, L. Inhibition of the NLRP3/caspase-1 signaling cascades ameliorates ketamine-induced renal injury and pyroptosis in neonatal rats. *Biomed Pharmacother* **2022**, *152*, No. 113229.
(37) Zhang, H.; Xu, R.; Wang, Z. Contribution of Oxidative Stress to HIF-1-Mediated Profibrotic Changes during the Kidney Damage. *Oxid. Med. Cell. Longevity* **2021**, *2021*, No. 6114132.
(38) Tang, Y.; Zhao, R.; Pu, Q.; Jiang, S.; Yu, F.; Yang, Z.; Han, T. Investigation of nephrotoxicity on mice exposed to polystyrene nanoplastics and the potential amelioration effects of DHA-enriched phosphatidylserine. *Sci. Total Environ.* **2023**, *892*, No. 164808.
(39) Shaw, P.; Chattopadhyay, A. Nrf2-ARE signaling in cellular protection: Mechanism of action and the regulatory mechanisms. *J. Cell Physiol.* **2020**, *235* (4), 3119−3130.
(40) Ungvari, Z.; Tarantini, S.; Nyúl-Tóth, Á.; Kiss, T.; Yabluchanskiy, A.; Csipo, T.; Balasubramanian, P.; Lipecz, A.; Benyo, Z.; Csiszar, A. Nrf2 dysfunction and impaired cellular resilience to oxidative stressors in the aged vasculature: from increased cellular senescence to the pathogenesis of age-related vascular diseases. *Geroscience* **2019**, *41* (6), 727−738.
(41) Ge, Y.; Lin, S.; Li, B.; Yang, Y.; Tang, X.; Shi, Y.; Sun, J.; Le, G. Oxidized Pork Induces Oxidative Stress and Inflammation by Altering Gut Microbiota in Mice. *Mol. Nutr. Food Res.* **2020**, *64* (2), No. e1901012.
(42) Andrade-Oliveira, V.; Foresto-Neto, O.; Watanabe, I. K. M.; Zatz, R.; Câmara, N. O. S. Inflammation in Renal Diseases: New and Old Players. *Front. Pharmacol.* **2019**, *10*, 1192.
(43) Tang, W.; Guo, J.; Liu, W.; Ma, J.; Xu, G. Ferrostatin-1 attenuates ferroptosis and protects the retina against light-induced retinal degeneration. *Biochem. Biophys. Res. Commun.* **2021**, *548*, 27−34.
(44) Yang, W. S.; Stockwell, B. R. Ferroptosis: Death by Lipid Peroxidation. *Trends Cell Biol.* **2016**, *26* (3), 165−176.
(45) Tsubouchi, K.; Araya, J.; Yoshida, M.; Sakamoto, T.; Koumura, T.; Minagawa, S.; Hara, H.; Hosaka, Y.; Ichikawa, A.; Saito, N.; Kadota, T.; Kurita, Y.; Kobayashi, K.; Ito, S.; Fujita, Y.; Utsumi, H.; Hashimoto, M.; Wakui, H.; Numata, T.; Kaneko, Y.; Mori, S.; Asano, H.; Matsudaira, H.; Ohtsuka, T.; Nakayama, K.; Nakanishi, Y.; Imai, H.; Kuwano, K. Involvement of GPx4-Regulated Lipid Peroxidation in Idiopathic Pulmonary Fibrosis Pathogenesis. *J. Immunol* **2019**, *203* (8), 2076−2087.
(46) Abdalkader, M.; Lampinen, R.; Kanninen, K. M.; Malm, T. M.; Liddell, J. R. Targeting Nrf2 to Suppress Ferroptosis and Mitochondrial Dysfunction in Neurodegeneration. *Front. Neurosci.* **2018**, *12*, 466.
(47) Song, X.; Long, D. Nrf2 and Ferroptosis: A New Research Direction for Neurodegenerative Diseases. *Front. Neurosci.* **2020**, *14*, 267.
(48) Yang, J.; Sun, X.; Huang, N.; Li, P.; He, J.; Jiang, L.; Zhang, X.; Han, S.; Xin, H. Entacapone alleviates acute kidney injury by inhibiting ferroptosis. *Faseb j* **2022**, *36* (7), No. e22399.
(49) Adedoyin, O.; Boddu, R.; Traylor, A.; Lever, J. M.; Bolisetty, S.; George, J. F.; Agarwal, A. Heme oxygenase-1 mitigates ferroptosis in renal proximal tubule cells. *Am. J. Physiol Renal Physiol* **2018**, *314* (5), F702−f714.
(50) Wang, X.; Zheng, X.; Zhang, J.; Zhao, S.; Wang, Z.; Wang, F.; Shang, W.; Barasch, J.; Qiu, A. Physiological functions of ferroportin in the regulation of renal iron recycling and ischemic acute kidney injury. *Am. J. Physiol Renal Physiol* **2018**, *315* (4), F1042−f1057.
(51) Chi, M.; Ma, K.; Wang, J.; Ding, Z.; Li, Y.; Zhu, S.; Liang, X.; Zhang, Q.; Song, L.; Liu, C. The Immunomodulatory Effect of the Gut Microbiota in Kidney Disease. *J. Immunol. Res.* **2021**, *2021*, No. 5516035.
(52) McIntyre, C. W.; Harrison, L. E.; Eldehni, M. T.; Jefferies, H. J.; Szeto, C. C.; John, S. G.; Sigrist, M. K.; Burton, J. O.; Hothi, D.; Korsheed, S.; Owen, P. J.; Lai, K. B.; Li, P. K. Circulating endotoxemia: a novel factor in systemic inflammation and cardiovascular disease in chronic kidney disease. *Clin J. Am. Soc. Nephrol* **2011**, *6* (1), 133−141.
(53) Cardinale, V.; Capurso, G.; Ianiro, G.; Gasbarrini, A.; Arcidiacono, P. G.; Alvaro, D. Intestinal permeability changes with bacterial translocation as key events modulating systemic host immune response to SARS-CoV-2: A working hypothesis. *Dig Liver Dis* **2020**, *52* (12), 1383−1389.
(54) Tian, S.; Zhao, Y.; Qian, L.; Jiang, S.; Tang, Y.; Han, T. DHA-enriched phosphatidylserine alleviates high fat diet-induced jejunum injury in mice by modulating gut microbiota. *Food Funct* **2023**, *14* (3), 1415−1429.
(55) Grosheva, I.; Zheng, D.; Levy, M.; Polansky, O.; Lichtenstein, A.; Golani, O.; Dori-Bachash, M.; Moresi, C.; Shapiro, H.; Del Mare-

https://doi.org/10.1021/acsomega.4c11437
ACS Omega 2025, 10, 7407−7421

Roumani, S.; Valdes-Mas, R.; He, Y.; Karbi, H.; Chen, M.; Harmelin, A.; Straussman, R.; Yissachar, N.; Elinav, E.; Geiger, B. High-Throughput Screen Identifies Host and Microbiota Regulators of Intestinal Barrier Function. *Gastroenterology* **2020**, *159* (5), 1807−1823.
(56) Kaya, D.; Kaji, K.; Tsuji, Y.; Yamashita, S.; Kitagawa, K.; Ozutsumi, T.; Fujinaga, Y.; Takaya, H.; Kawaratani, H.; Moriya, K.; Namisaki, T.; Akahane, T.; Yoshiji, H. TGR5 Activation Modulates an Inhibitory Effect on Liver Fibrosis Development Mediated by Anagliptin in Diabetic Rats. *Cells* **2019**, *8* (10), 1153.
(57) Inserra, A.; Rogers, G. B.; Licinio, J.; Wong, M. L. The Microbiota-Inflammasome Hypothesis of Major Depression. *Bioessays* **2018**, *40* (9), No. e1800027.
(58) Yoshifuji, A.; Wakino, S.; Irie, J.; Tajima, T.; Hasegawa, K.; Kanda, T.; Tokuyama, H.; Hayashi, K.; Itoh, H. Gut Lactobacillus protects against the progression of renal damage by modulating the gut environment in rats. *Nephrol Dial Transplant* **2016**, *31* (3), 401−412.
(59) Heeney, D. D.; Gareau, M. G.; Marco, M. L. Intestinal Lactobacillus in health and disease, a driver or just along for the ride? *Curr. Opin Biotechnol* **2018**, *49*, 140−147.
(60) Iljazovic, A.; Roy, U.; Gálvez, E. J. C.; Lesker, T. R.; Zhao, B.; Gronow, A.; Amend, L.; Will, S. E.; Hofmann, J. D.; Pils, M. C.; Schmidt-Hohagen, K.; Neumann-Schaal, M.; Strowig, T. Perturbation of the gut microbiome by Prevotella spp. enhances host susceptibility to mucosal inflammation. *Mucosal Immunol* **2021**, *14* (1), 113−124.
(61) Yang, J.; Kim, C. J.; Go, Y. S.; Lee, H. Y.; Kim, M. G.; Oh, S. W.; Cho, W. Y.; Im, S. H.; Jo, S. K. Intestinal microbiota control acute kidney injury severity by immune modulation. *Kidney Int.* **2020**, *98* (4), 932−946.
(62) Nakade, Y.; Iwata, Y.; Furuichi, K.; Mita, M.; Hamase, K.; Konno, R.; Miyake, T.; Sakai, N.; Kitajima, S.; Toyama, T.; Shinozaki, Y.; Sagara, A.; Miyagawa, T.; Hara, A.; Shimizu, M.; Kamikawa, Y.; Sato, K.; Oshima, M.; Yoneda-Nakagawa, S.; Yamamura, Y.; Kaneko, S.; Miyamoto, T.; Katane, M.; Homma, H.; Morita, H.; Suda, W.; Hattori, M.; Wada, T. Gut microbiota-derived D-serine protects against acute kidney injury. *JCI Insight* **2018**, *3* (20), No. e97957.
(63) Liu, Z.; Xu, B.; Ding, Y.; Ding, X.; Yang, Z. Guizhi Fuling pill attenuates liver fibrosis in vitro and in vivo via inhibiting TGF-beta1/Smad2/3 and activating IFN-gamma/Smad7 signaling pathways. *Bioengineered* **2022**, *13* (4), 9357−9368.

https://doi.org/10.1021/acsomega.4c11437
ACS Omega 2025, 10, 7407−7421